Numerical simulation of shock events and associated response of satellite

Tess Legaud[1], Nicolas Van Dorsselaer[1], Vincent Lapoujade[1], Simon Lemay[1]

[1] Dynas+, 5 Av. Didier Daurat, 31400 Toulouse, France
[2] CNES Toulouse (National Centre for Space Studies), 18 avenue Édouard Belin, 31401 Toulouse

1 Abstract

The paper presents CNES' and Dynas+ partnership recent activities to improve shock events simulation and predict shock propagation in structures and equipment. The last activities presented here have been focused on shock test prediction by numerical analysis (i.e. virtual shock testing). The simulations were performed using LS-DYNA®, whereas the use of explicit non-linear computation codes is not common in the space industry to deal with spacecraft mechanical environments. Especially, the activities aimed at modelling physically the shock event generated by one of CNES' pyrotechnic test device and to predict the acceleration levels generated by this source on the structural model of a microsatellite. To do so, multiple intermediate steps had to be studied, beginning by the modelling of a simple sphere impacting a plate. The model complexity increased progressively to reach the modelling of a satellite vibrations induced by shock sources. In order to assess model predictability, all the tests were performed at various shock energies and compared to experimental results.
This paper will present the results and comparisons with experimental SRS (Shock Response Spectrum) obtained starting with "simple" cases up to cases integrating complex structures and shock sources.

2 Introduction

Among the various mechanical environments that a spacecraft must withstand (sine and random vibrations, acoustics, thermoelastics…) the shock environment is probably the least mastered by the space community. Especially, numerical analyses are rarely performed for shock environments because they are distinctly less reliable and predictive than for other mechanical environments. Thereby, shock resistance justification is usually performed exclusively by tests that occur late in the project. However, most of the time, no sizing to this environment or test prediction analyses were performed. This methodology presents a high risk of failure with potentially severe consequences on project planning and cost.

CNES' pyrotechnics laboratory performs shock tests using two pyrotechnically actuated impact test benches. The ESA/CNES shock test bench is a pyrotechnic cannon associated with a bi-plate able to generate high acceleration levels (up to 10 000g SRS at 1000 Hz) with high frequency content. This test device dynamic behaviour is well known and is dominated by the bi-plate's response. It is however limited to the testing of small equipment.

Another shock test device has been developed at CNES for the last few years and is continuously being improved. The PSG (PyroShockGun) is a portable shock generator. It is made to be fastened, through an interface part, to the structure to be tested (i.e. there is no test bench). The load generated by the PSG, and so the acceleration levels generated, are very dependent on the mass and dynamic behaviour of the structure tested and on the interface stiffness between the PSG and the structure. This strong coupling between the shock generator and the structure to be tested makes the shock levels very difficult to predict.

Specific tests and numerical models were built to try to predict the shock levels generated by one or several PSGs, depending on the structure tested. To achieve that objective, a step-by-step approach was implemented. Each step consisted in performing a shock test and making a representative numerical model of that test. The idea was to start with very simple case studies and to increase very progressively the complexity of the tests and models. Moreover, the CNES wanted the models to be simple and representative of their usual mechanical models used in Nastran® modal analysis. The idea was to develop a complete shock modelling methodology enabling the Nastran modal model conversion to an LS-DYNA shock model.
To do so, the following tests and models were realised and are presented in this paper:

- Impact of a steel ball on an aluminium plate

- *Impact of a steel ball on an aluminium plate with a simple 3D part screwed on it*
- Impact of a steel ball on a machined aluminium 3D part (bottom panel of a microsatellite)
- Impact of a steel ball on an aluminium sandwich panel
- PSG shock test on an aluminium plate
- PSG shock test on a sandwich panel
- PSG shock test on the structural model of a microsatellite

All the presented simulations were performed with LS-DYNA. Only the case in italic is not presented in this paper. This work was already presented in [1] and this publication has to be considered as an enrichment of results and numerical descriptions.

3 Steel balls impacts

The steel balls were initially modelled by solid elements associated to a non-deformable behaviour using ***MAT_RIGID** [2].

3.1 Drop on an aluminium plate

3.1.1 Tests & simulations configurations

The test set-up for that first elementary case study is presented in the figure below. The set-up consisted in a 560x535x13mm (11kg) aluminium plate laid on very soft foams and impacted in its centre by various steel balls with various speeds. The aluminium plate is modelled by fully integrated shell elements associated to a bilinear behaviour implemented in the ***MAT_PIECEWISE_LINEAR_PLASTICITY** law. Since the foams between the plate and the ground were very soft, the numerical models considered that the induced boundary conditions were totally free. A simulation representing the foams has still been performed in order to validate this hypothesis.
The following load cases, depending on the ball's diameter, mass and impact speed were tested and simulated:

- 255.5g (39.7mm) at 1.72m/s (0.38J)
- 255.5g (39.7mm) at 2.43m/s (0.75J)
- 255.5g (39.7mm) at 3.43m/s (1.5J)
- 358g (44.4mm) at 2.43m/s (1.05J)
- 535g (50.8mm) at 2.43m/s (1.57J)

The speeds were determined by the drop height and implemented in the numerical model using the keyword ***INITIAL_VELOCITY_RIGID_BODY**.
Five mono-axis accelerometers (two at the shock source, two at the middle of edges and one in a corner) measuring out of plane accelerations were used. Those accelerometers were modelled by ***ELEMENT_SEATBELT_ACCELEROMETER**. In order to be able to compare experimental and numerical SRS with equivalent spectrum discretisation, the output frequencies of the numerical accelerometers have been adapted. Moreover, the simulations were performed on 100ms to obtain a sufficient studied frequency range.

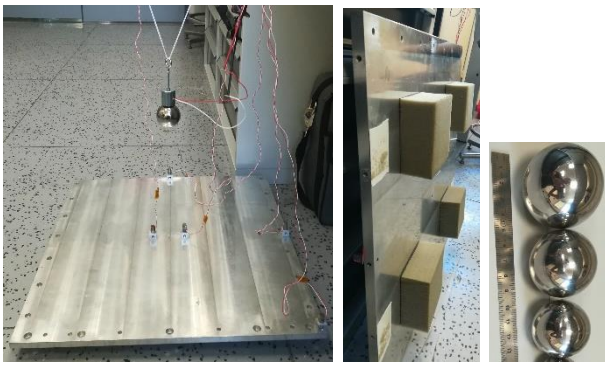

Fig. 1: Steel ball impact on an aluminium plate test set-up

The interaction between the balls and the plate is modelled by a ***CONTACT_AUTOMATIC_SURFACE_TO_SURFACE** with SOFT=1 and a friction coefficient of 0.1.

3.1.2 Results

The figure below shows the comparison between experimental and numerical SRS results obtained for the lowest energetical case, given by two accelerometers: one near the shock source (Acc 2) and one

far from it, near a plate corner (Acc 5). This figure shows the results obtained with the initial model, compared to the ones obtained with an “optimized” one, reached after some iterations. This last one considered, among others, a deformable steel impactor (instead of rigid one) and a timestep divided by 10 during the contact duration between the ball and the plate.

	Initial model	“Optimized” model
Acc 2 (near shock source)	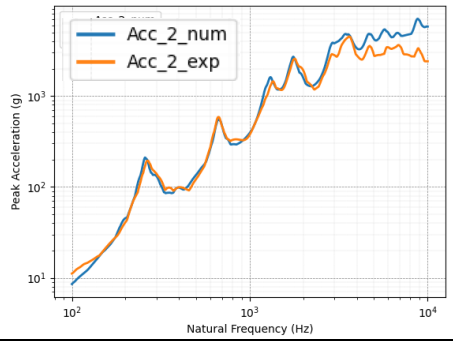	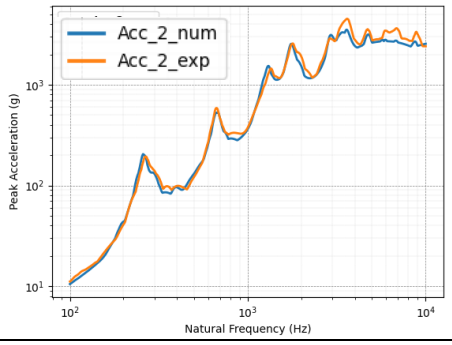
Acc 5 (far from shock source)	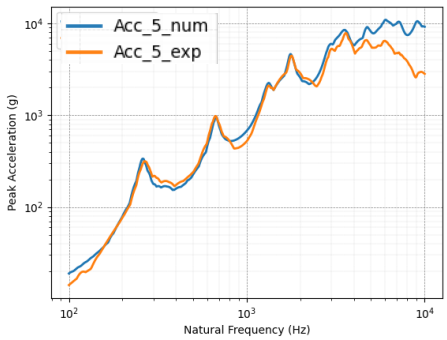	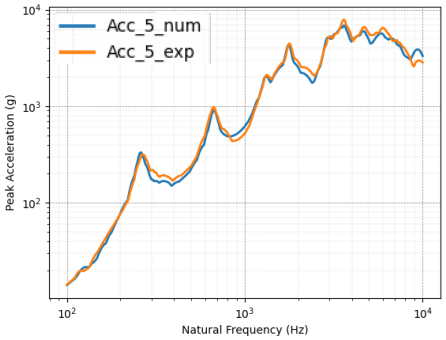

Fig. 2: Comparison of the test and simulation SRS for accelerometers 2 and 5 given by the initial model and the “optimized” one – lowest energy case

The optimized model enables a good correlation since the committed error is inside the accepted range [-3dB, 3dB]. In order to validate the simulation method established on this load case on a larger range of load intensity, the same model has been performed including variations of ball mass (diameter) and drop high. The figure below shows the SRS given by the most energetical load case.

	Acc 2 (near shock source)	Acc 5 (far from shock source)
SRS (g)	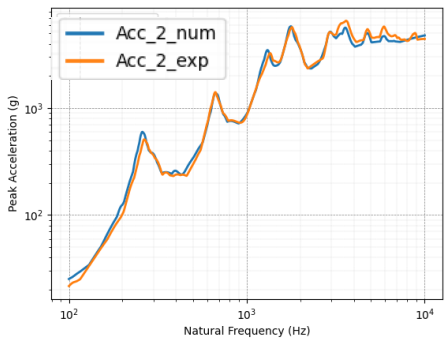	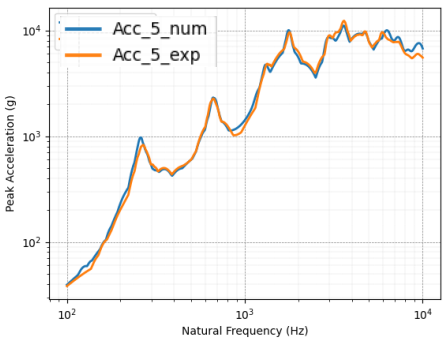

Error spectrum (dB)	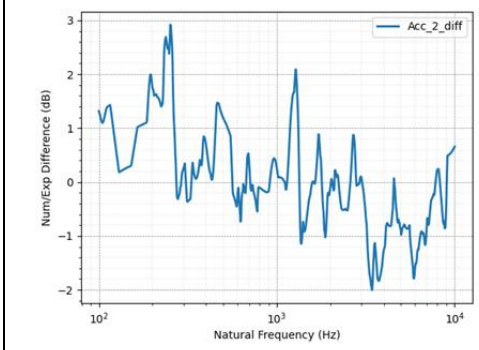	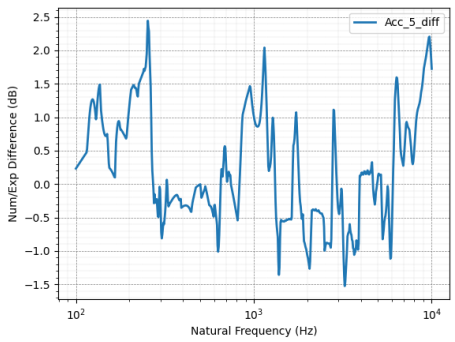

Fig. 3: Comparison of the test and simulation SRS for accelerometers 2 and 5 – highest energy case

Again, we observe a good correlation between experiments and simulations, traduced by a respected error range of [-3dB, 3dB]. The other load cases provided the same kind of encouraging results, so that the test case complexity could be increased.

3.2 Drop on a bottom panel (-X) of a microsatellite

3.2.1 Tests & simulations configurations

This second case study is dedicated to the propagation of the shock in a large and massive machined aluminium part (544x573mm and 8.3kg), representative for the bottom panel of a microsatellite platform. The shock is generated by the same steel balls than for the first case study. The test set-up and the instrumentation, which consisted in 8 mono-axis out-of-plane accelerometers, are presented in the figure below as well as the numerical model.

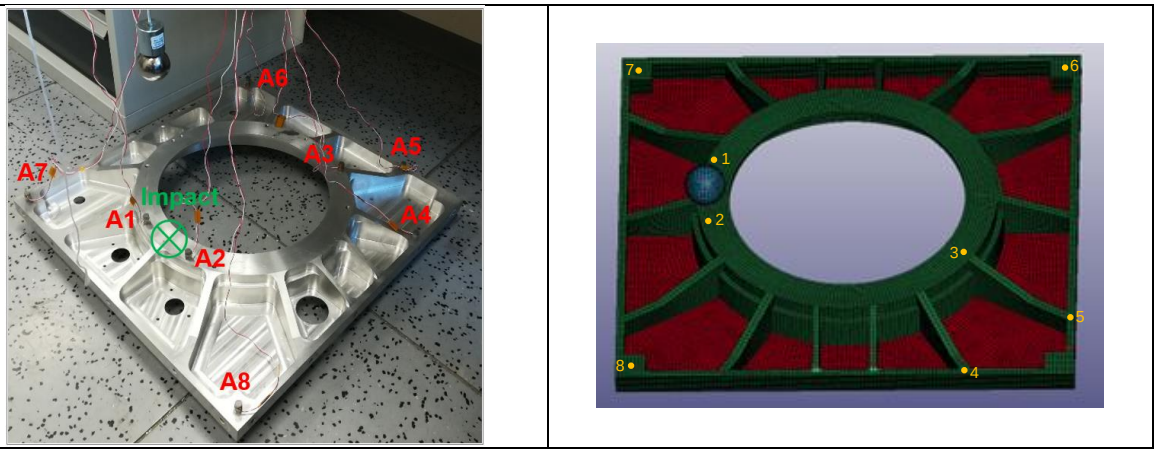

Fig. 4: Steel ball impact on a machined aluminium panel test set-up

The mesh is a mix of linear fully integrated hexahedral elements (in red) and linear fully integrated shell elements (in green). The ball is meshed in 3D and steel elastic material properties are associated to it as in the previous test case model. The elasto-plastic material model for the plate is the same as the one used in previous case studies. The mesh size is about 5mm or less. The same loads, contact and boundary conditions are applied to the ball and the panel as the ones used in the previous test case model. The same goes for the global modelling methods established in part 3.2. The accelerometers positions are localized by the red or yellow points on the figure upward.

3.2.2 Results

The results obtained with this model are presented in the figure below for a 255g ball dropped from 0.15m

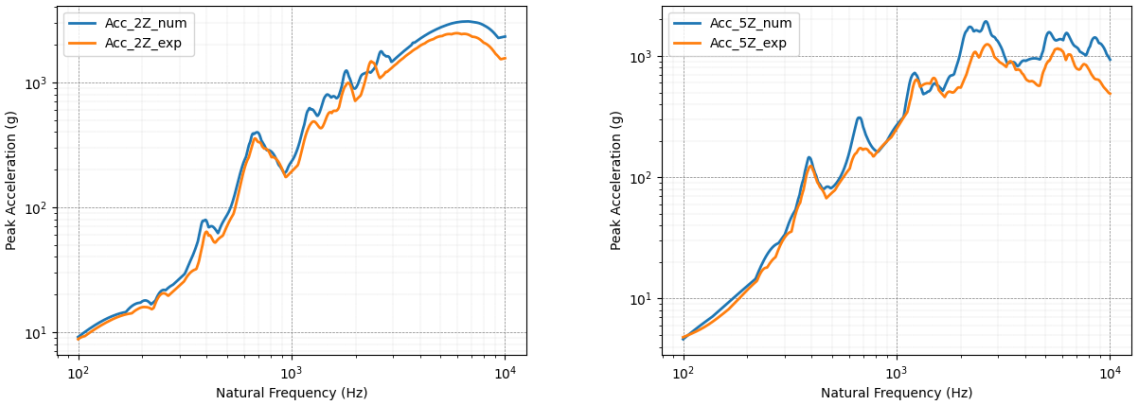

Fig. 5: Comparison of the test and simulation SRS for accelerometers 2 and 5 – 255g ball drop from 0.15m

The comparison of the numerical simulation results with the test results is satisfying on all accelerometers. The correlation is slightly less satisfying than for the simple plate but considering the greater complexity of this part it is very correct.

3.3 Drop on aluminium sandwich panel

3.3.1 Tests & simulations configurations

This 3rd case study consists in an aluminium sandwich panel impacted by the same steel balls as for the previous ones. In order not to damage the sandwich panel, the impact occurs on an assembly of one aluminium and one steel part screwed in four M5 inserts in the sandwich panel. The two aluminium and steel parts are linked by one M8 screw. The test configuration and the associated model are shown in the figure below.

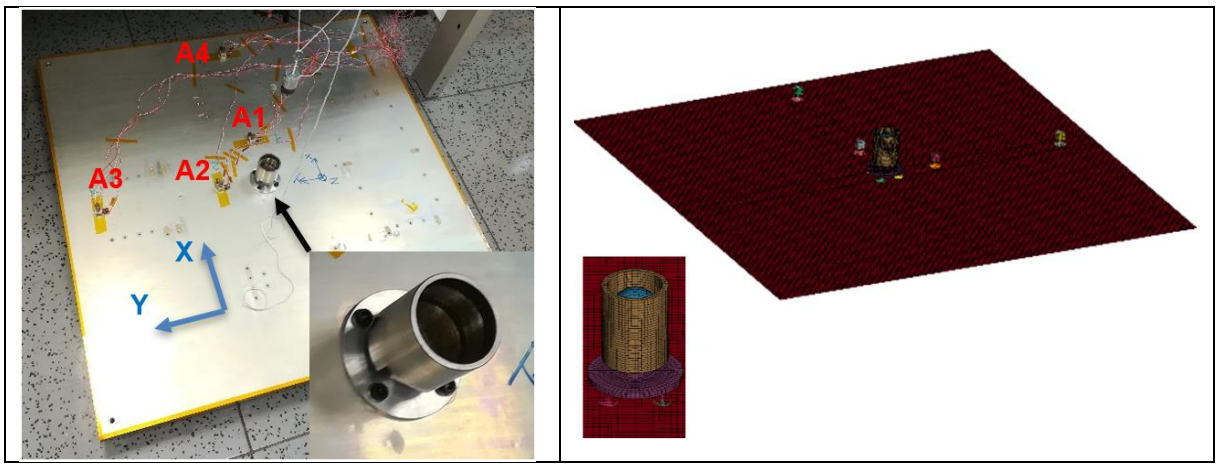

Fig. 6: Ball drop on a sandwich panel experimental set-up, accelerometers locations and associated model

The characteristics of the sandwich panel are the following:

- Dimensions: 1x1x0.025m
- Skins: 0.3mm thick 2024 aluminium
- Nida: Hexcel 5/32 5056 0.001

The instrumentation consisted in 4 tri-axes accelerometers (4 x 3 mono-axis accelerometers screwed on an aluminium cube glued on the panel). The figure below shows a tri-axis accelerometer glued on the sandwich panel.

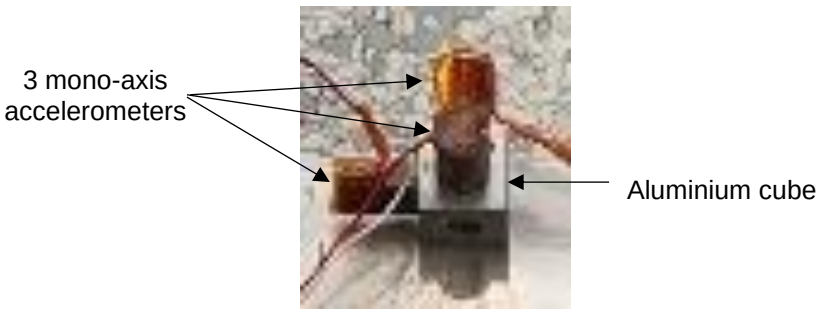

Fig. 7: View of a tri-axial accelerometer assembly

The first difficulty of this case was to correctly model the sandwich panel behaviour. Since the honeycomb cells are too small to be represented, an orthotropic homogenised behaviour law was used. Multiple LS-DYNA materials were tested, and in accordance with the available mechanical data, ***MAT_COMPOSITE_FAILURE** was finally chosen. The sandwich panel was then defined by a ***PART_COMPOSITE**, containing two external elastoplastic aluminium skins and an orthotropic honeycomb core.
The second difficulty consisted in correctly simulating the multiple connections (steel part/aluminium part, aluminium part/sandwich panel, accelerometers/sandwich panel). Indeed, it appeared that the way to model those connections was a critical parameter influencing the numerical results varying the correlation quality.
The final connections modelling strategy concerning the drop test of a ball on the sandwich panel is given below:

- Screws are modelled with beams, and the area affected by the aluminium insert enabling the screwing in the sandwich panel is made rigid through the creation of a ***CONSTRAINED_NODAL_RIGID_BODIES** (CNRB),
- Contacts with option SOFT=2 are used between the ball and the steel part, and between the accelerometers and the sandwich panel,
- A tied contact is created between the steel part and the aluminium one,
- The connection between the tri-axis accelerometers and the plate was adjusted in the previous simplest test case involving the drop of a ball on the aluminium plate. This connection consisted in the modelling of each screw by a beam element, since the accelerometers are screwed and not glued in this previous test case. The aluminium cubes had to be deformable, and a penalty contact had to be defined between the accelerometers and the plate.
  After some tests, the same modelling as in the one coming from the simplest case described in this paragraph has been used in the current test case (that means that the accelerometers are not tied but modelled screwed even if they were glued on the panel experimentally).

3.3.2 Results

The simulation results compared to the test measures are presented in the following figure for a 255g steel ball dropped from 0.3m.

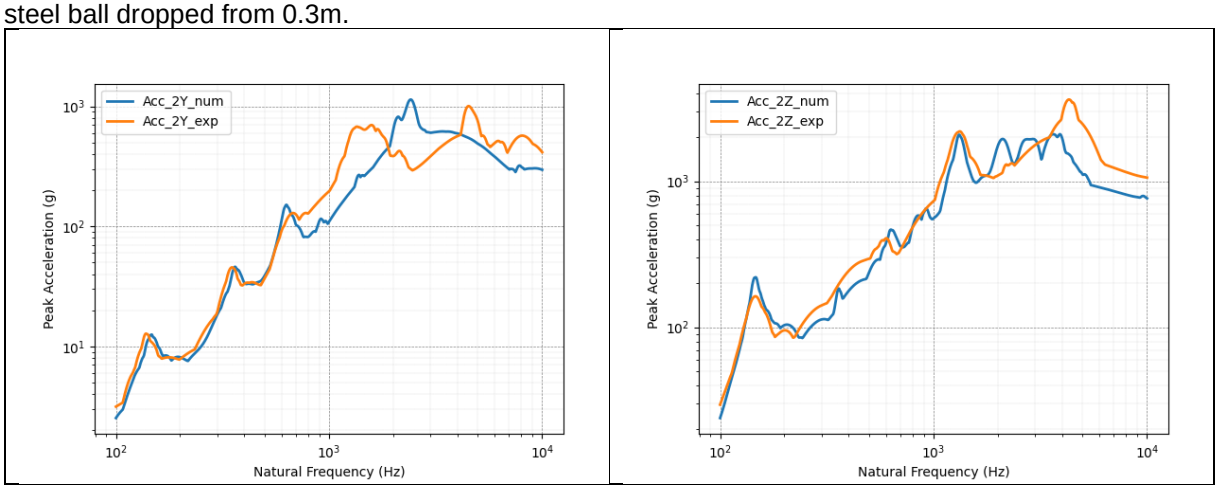

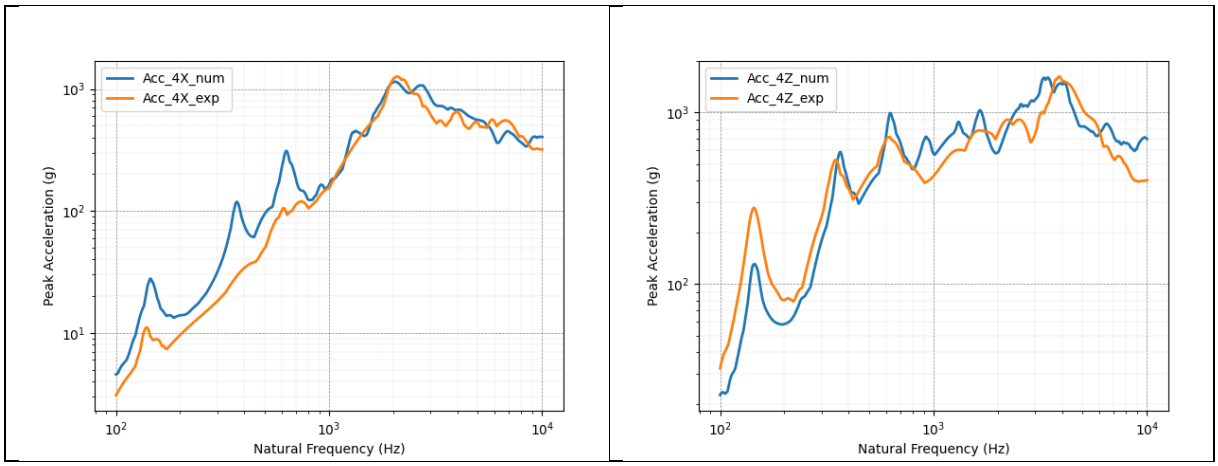

Fig. 8: Comparison of the test and simulation SRS for accelerometers 2 and 4 in in-plane and out-of plane directions – 255g ball drop from 0.3m

The correlation is globally correct but the accuracy of the model is significantly lower than for the previous case studies. Especially, local amplifications at particular frequencies exist in the model and not in reality. In addition, the first plate mode is amplified or underestimated in far field accelerometers (A4 presented here for example). These results are very encouraging considering the problem (shock propagation in a complex sandwich structure surmounted by multiple connected parts) and model used (simple 2D equivalent representation) but could probably be improved and need more work effort.

4 PSG shocks

For the following case studies, the shock source is no longer a steel ball accelerated by gravity but a PSG, a real shock test mean. This PSG works as a non-destructive firearm and is an assembly of some fixed and mobile parts that have to transmit a defined shock to the fastened structure. Multiple shock energies can be generated and studied by this experimental device created by CNES. The main parts of the PSG were modelled and some of those motionless parts connections were simplified and modelled with merged nodes.
This device also implies the use of a polymeric cylindrical damper whose behaviour modelling was part of the tricky sensitivity study, since no mechanical data were available to correctly describe its behaviour. For each studied energy shock generated by the PSG, a set of mechanical properties, resulting in a bilinear elasto-plastic curve, had to be fitted since we knew that this material behaviour depends on strain rate. Moreover, the highest shock tests led to this damper failure (more or less widespread) which was another modelling difficulty. This failure modelling has been tested but without success during this global study. To go further, a strain rate effects characterization of the damper material could be a great help for the models improvement.

4.1 Shock on the aluminium plate

4.1.1 Tests & simulations configurations

The PSG is fastened to the same plate as the one used for the first case study (§3.1) through one M10 screw. This one is modelled by a beam which base on the plate is made rigid by a CNRB whose diameter is 10mm. The following figure presents the experimental configuration and the associated model. The instrumentation of the test is as follows, and the accelerometers modelling is identical to the one described in previous sections:

- 3 mono-axis: A1, A2, A4,
- 2 tri-axes: A3 and A5.

Fig. 9: PSG on a plate experimental set-up, accelerometers locations and associated model

As explained previously, the most of the correlation effort done on those models consisted in finding the appropriate damper bilinear behaviour law. However, multiple sensitivity tests were led, particularly on the interactions between parts. Finally, it appeared that avoiding the contact between the PSG bottom and the plate led to a better fitting, so the main part of the force generated by the PSG was transmitted to the plate through the M10 screw. The use of an additional contact led to a too much stiff behaviour traduced by overestimated accelerations at high frequencies.

4.1.2 Results

Four energy shock configurations were modelled, and two of them are presented here: the lowest and the highest energy cases. The following figure shows the results obtained for the lowest and highest energies cases.

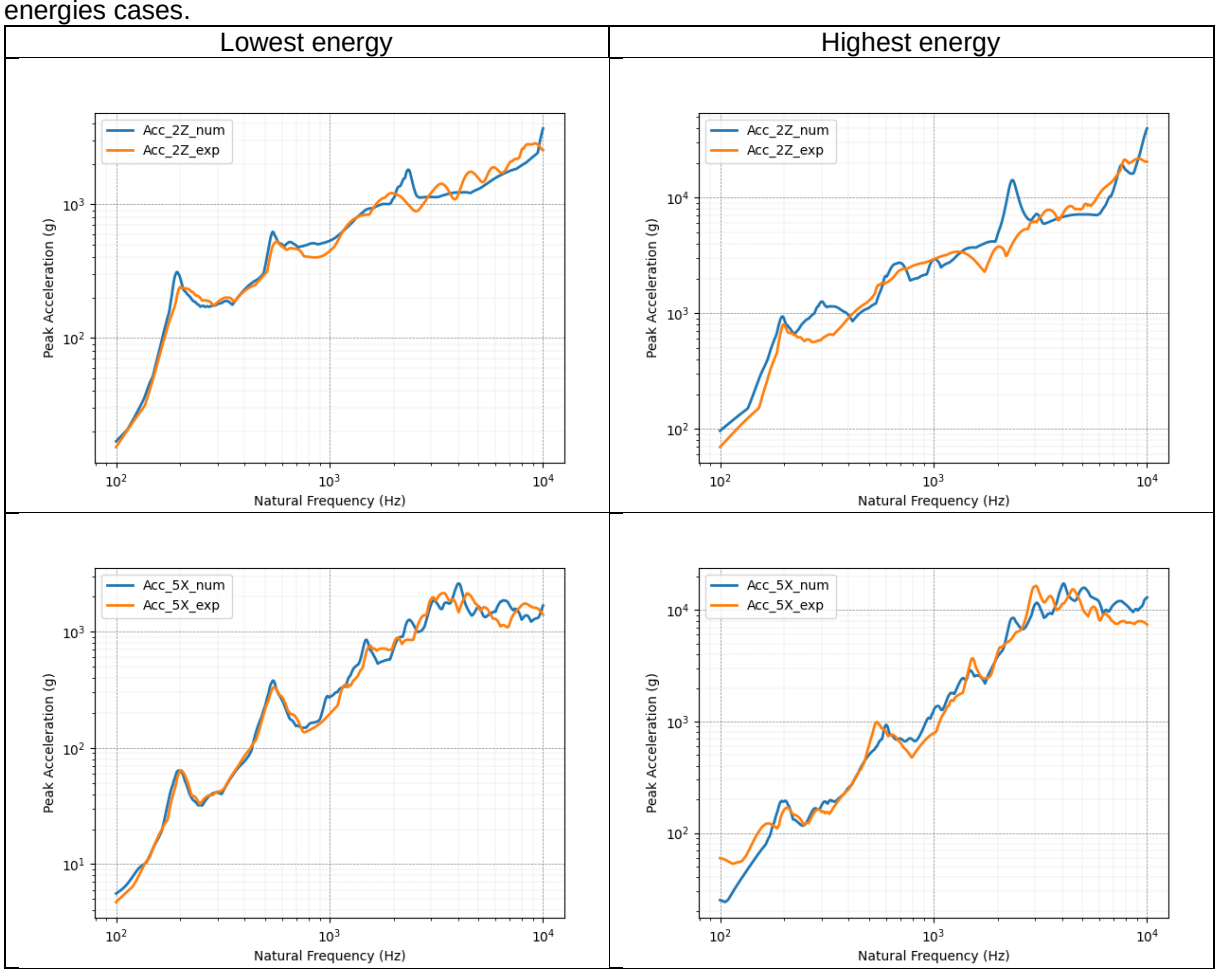

Fig. 10: Comparison of the test and simulation SRS for accelerometers 2Z and 5X – lowest and highest energies

Those results show that it is possible to obtain a good correlation between the model and test in terms of SRS acceleration without modelling accurately the deformation of the damper in a “simple” test case. The correlation is satisfying on all accelerometers, in-plane and out-of-plane. The PSG model for those settings can be considered quite mature to go further in complexity, since the only modifications in the model between each energy case concerned the damper behaviour law. Knowing that, we made the hypothesis that the modelling methods (interactions, CNRB strategy, timestep, etc) was repeatable and reliable to be used in a more complex configuration.

4.2 Shock on an aluminium sandwich panel

4.2.1 Tests & simulations configurations

This case study consists in the same sandwich panel than presented in §3.3. but shocked by a PSG instead of a steel ball. The test configuration with its instrumentation and the model are presented in figure below.

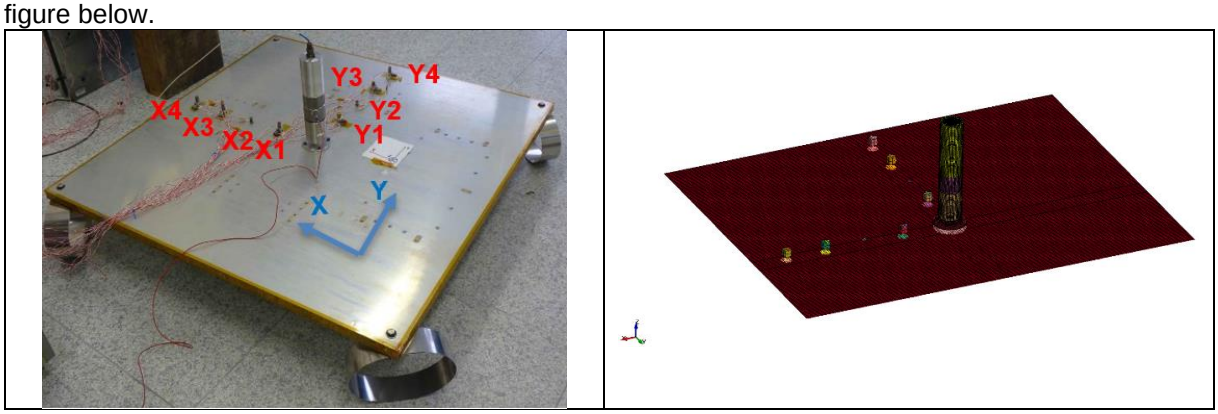

Fig. 11: PSG on a sandwich panel experimental set-up, accelerometers locations and associated model

As described in the §3.3, the bottom of the PSG is fastened to an aluminium connection part, screwed on the sandwich panel with 4 M6 screws. After a series of test, it appeared that the best connection set is as follows:

- All the panel nodes located under the connection part are linked together by a CNRB,
- No contact definition between the connection part and the panel,
- The connection part and the bottom of the PSG are tied together.

4.2.2 Results

The following figures show the SRS obtained in nearby field (Y1) and in far field (X4) for the highest energy case.

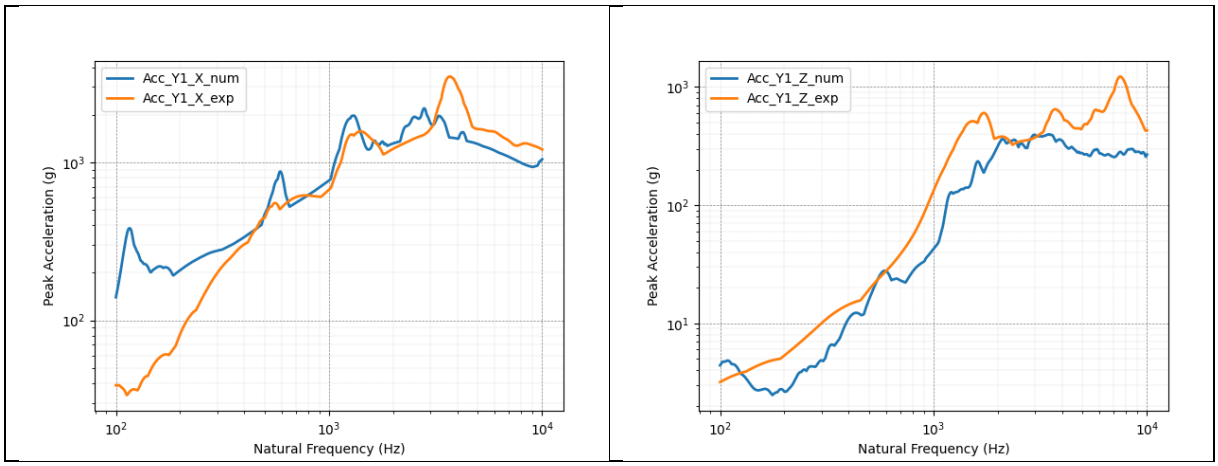

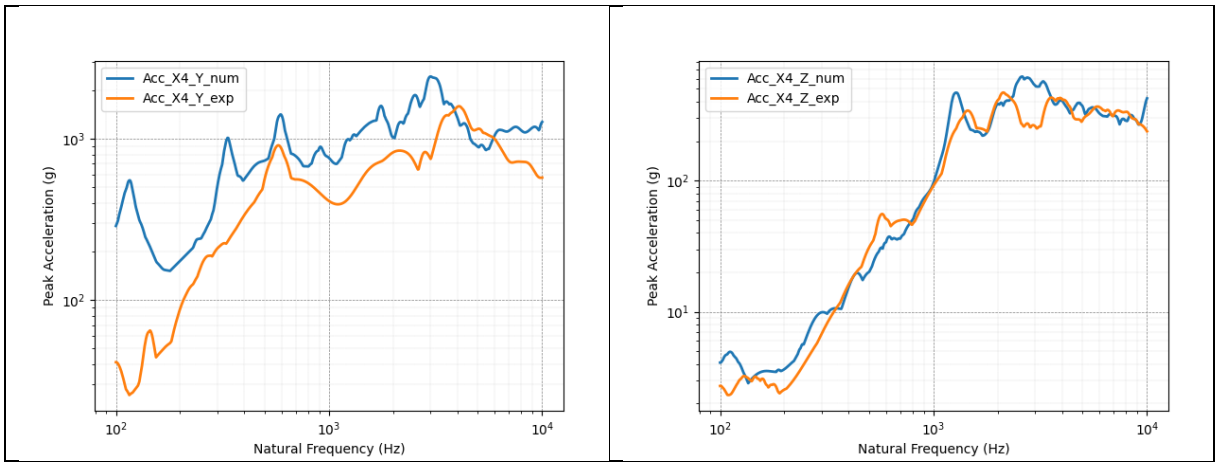

Fig. 12: Comparison of the test and simulation SRS for accelerometers Y1 and X4 in in-plane and out-of plane directions – highest energy

The more the case complexity increased, the more the simplification hypothesis might have influence on the numerical results and led to fitting difficulties. Moreover, on the SRS there are two main range of frequencies:

- The high frequencies correspond to the ones excited by the shock and are detected and well measured by the accelerometers during the first 20ms.
- The low frequencies correspond to the global modes of the assembly and are excited during a longer duration. In order to well measure them, the computations have to go until 100ms.

Because of the numerical hypothesis (connections/interactions, materials definitions), it was quite hard to obtain good agreements on nearby field accelerometers at the same time as far field ones on all the studied spectrum.
This is what is shown here: the far field accelerometer (X4) gave a good agreement with the test in out-of plane measurement. However, with this modelling, the nearby field accelerometer (Y1) underestimates the accelerations in the complete spectrum.
Next, Y1 in-plane measurement give good agreements with test at medium and high frequencies, whereas the low frequencies (panel oscillating frequencies) are too much overestimated. X4 in-plane measurement overestimates all the spectrum, even if medium and high frequencies show an encouraging spectrum tendency. The bad measurement of the low frequencies might come from the modelling of the sandwich panel, since natural frequencies are directly linked to the material moduli.
Again here, considering the case complexity, those results were considered acceptable, and could be improved by a further material behaviour and connections study.

4.3 Shock on the structural model of Microcarb

4.3.1 Tests & simulations configurations

The last case study is the shock calibration tests of Microcarb satellite on a structural model. The main goal of the tests was to define the test configuration, (i.e. the interface structure between the PSG and the satellite) and the PSG settings in anticipation to the shock qualification tests of the PFM Microcarb Payload Module (PLM) to the launcher shock. Various configurations (different interface plates, direct mounting of the PSGs on the satellite interface ring (SIR), different PSG positions and orientations…) were tested to demonstrate that the chosen one would allow reaching the qualification levels for the PFM PLM test. The second objective of the test was to characterise shock transfer functions inside the platform to define specifications for some platform equipment.
The main benefits of carrying shock test predictions of such a test are:

- Anticipate any problem, for example an under sizing of the test mean with respect to the specification to achieve,
- Define the test configuration by numerical analysis (i.e. specific interface design),
- Define a representative PLM dummy by numerical analysis or at least estimate the differences to be expected between the calibration and the qualification test,
- Identify early potential shock problems for equipment.

These reasons lead us to carry out this study to investigate the possibility of performing shock test predictions by numerical analysis, what requires modelling physically the shock source. This was the main objective of the previous case studies.

The original Nastran FE model of the structural model of Microcarb developed by CNES was converted to LS-DYNA and the PSG were added. The configuration simulated includes a 35mm thickness plate screwed on the satellite interface ring and four PSGs oriented in the out-of-plane direction are linked to this thick plate through the use of four cylindrical plates, as presented in the following figure.

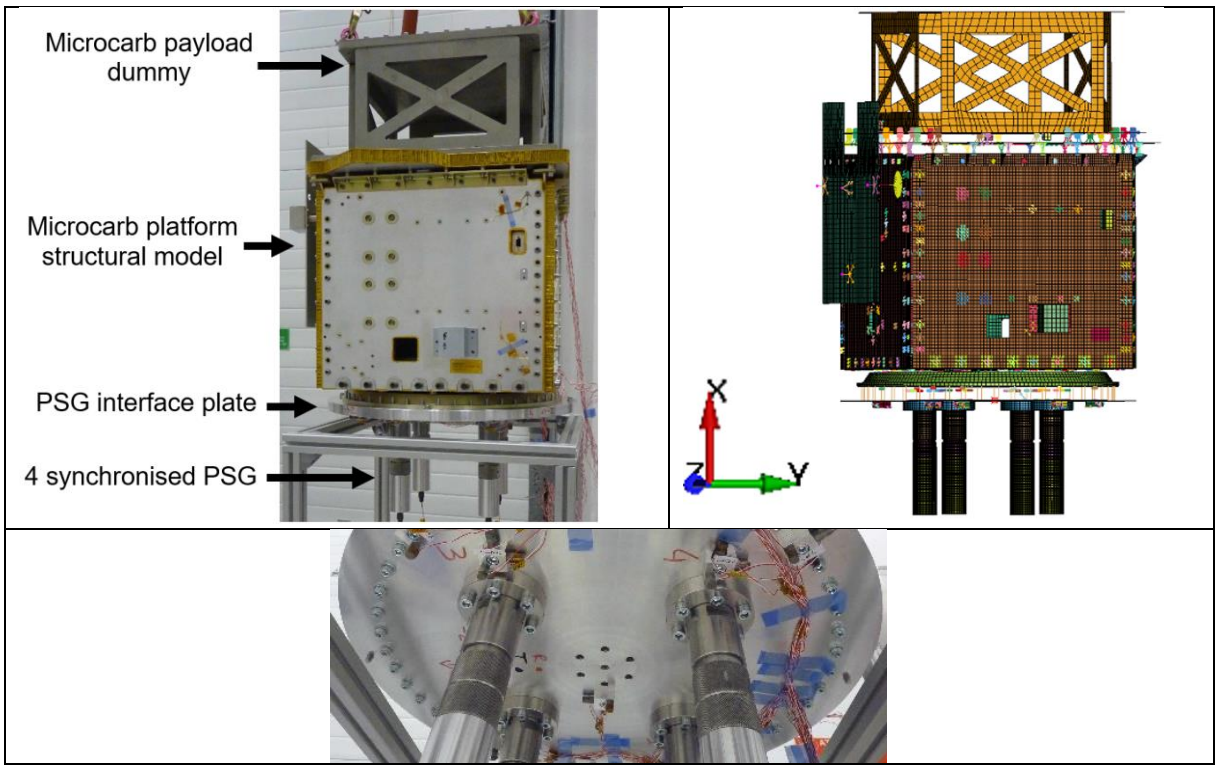

Figure 26: Microcarb launcher shock calibration tests configuration, PSG set-up to simulate the shock transmitted by the launcher & LS-DYNA FE model of the shock test configuration

As presented in the previous cases, the addition of interface parts corresponds to an increasing model complexity and to more potential fitting difficulties. So multiple tests were led in order to identify an acceptable interfaces management. The final strategy consists in not taking into account the various contacts between the SIR, the thick plate, the four cylindrical plates and the PSGs. All the forces went through the linking screws modelled with beam elements associated to CNRB at their base. No contact was defined in the satellite model traduced from Nastran, since the objective was to keep it unchanged as much as possible.
The PSG modelling and the accelerometers one were kept from previous cases.
No boundary conditions are applied to the payload.

4.3.2 Results

The following figures show the SRS obtained in the 2 directions from an accelerometer at the shock source for the highest and lowest energy cases. The optimised model exclusively integrated modifications in terms of interactions management and areas dimensions made rigid at the bottom of the beam elements.

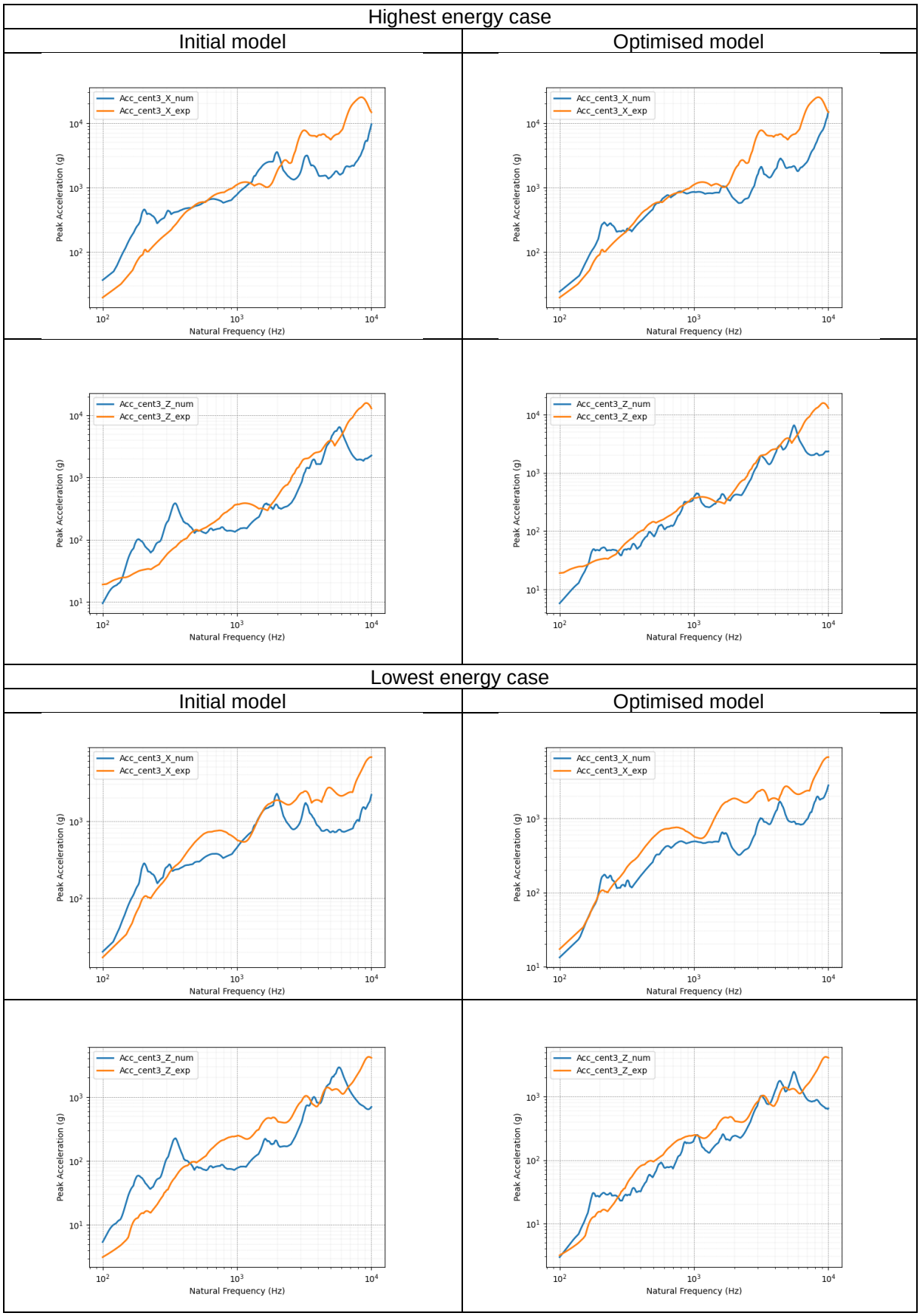

Fig. 13: Comparison of the test and simulation SRS for accelerometer CENT3 (X, Z) given by the initial model and the optimized one – highest and lowest energy

The following figures show the SRS obtained in the out of plane direction from an accelerometer on a lateral panel for the highest and lowest energy cases.

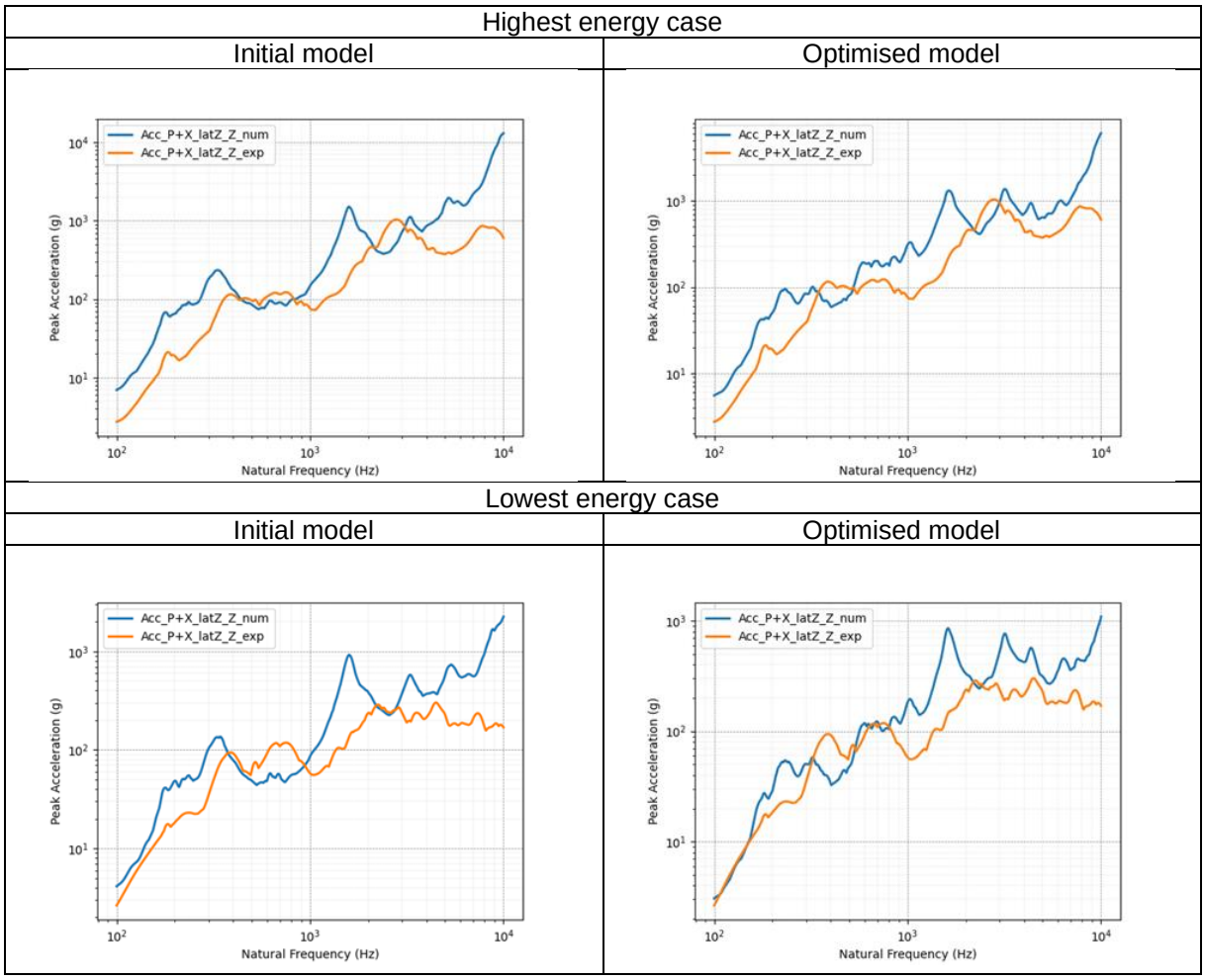

Fig. 14: Comparison of the test and simulation SRS for accelerometer P+X_latZ (X, Y, Z) given by the initial model and the optimized one – highest and lowest energy

In both results sets, it is observable that the way the interactions are managed and the dimensions of the rigid areas at the beams bases have a huge influence on all the studied spectrum, as long as on the accelerometer position and measurement direction.
Moreover, the accelerometers located at the shock source gave better fittings than the one located far from it. It is important to notice that those far accelerometers are located on sandwich panels, and it has been seen in the previous case that we encountered difficulties to reproduce accurately the shock induced oscillations of such panel.
It is obvious that the fittings presented here are less satisfying than the one obtained in the previous cases. However, this kind of model is much more complicated and involves a lot of parts interactions which exacerbate the difficulties. Since the LS-DYNA model came directly from a translation of the Nastran one which was tuned to fit the experimental modal tests and used for modal analyses, it is conceivable that the natural frequencies of the LS-DYNA model do not correspond exactly to the one identified by Nastran. A modal fitting between the experiment and the LS-DYNA model could be a first idea to improve the results. Coming from such work, the model of the satellite should probably not be the same as the one issued from Nastran.
Moreover, a better representation of the PSG damper should improve the results.
After that, it should be really interesting to perform a LS-OPT analysis enabling the such shock models main parameters optimization on the three cases at the same time.

5 Summary

The activities performed in the frame of that study allowed, step-by-step, to perform a shock test prediction using only the physical parameters of the test mean. The activities started voluntarily with very simple cases in order to learn good practices to model the generation and propagation of the shocks of interest. The results obtained are encouraging and allow imagining further activities to develop robust and predictive shock numerical models since multiple improvement methods have been identified.

6 Literature

[1] Lemay S., Doulsier G., Gallet R., Raynal E., Legaud T., Van Dorsselaer N.: "Numerical Simulation of the Generation and Propagation of Pyrotechnic Shocks for Shock Test Prediction", 17th ECSSMET, 2023

[2] Ansys LST, “LS-DYNA User’s Manual”, 2020